Reports

Melting of Diamond at High Pressure

GIULIA GALLI,* RICHARD M. MARTIN, ROBERTO CAR,
MICHELE PARRINELLO

Melting of diamond at high pressure and the properties of liquid carbon at pressures greater than 1 megabar were investigated with a first-principles molecular dynamics technique. The results indicate an increase of the diamond melting temperature with pressure, which is opposite to the behavior of silicon and germanium. This is contrary to long-held assumptions, but agrees with recent experiments, and has important implications for geology and astrophysics. As is the case for the solid phase of carbon at low temperature, which changes greatly with pressure from graphite to diamond, the structural and bonding properties of liquid carbon vary strongly with pressure.

THE PHASE DIAGRAM OF C HAS BEEN the subject of active research for several decades in fields such as condensed matter physics (*1*), geology (*2–4*), and astrophysics (*5*). Unfortunately, progress has been slow. The key experimental problem is the extreme temperature required to melt both diamond and graphite; on the theoretical side a comprehensive model that describes the complex bonding properties of C as a function of temperature (T) and pressure (P) has long been lacking.

The graphite-diamond phase boundary and the graphite melting curve are the only lines of the phase diagram that seem to be well established (*1*). However, whether graphite melts directly or first transforms to an intermediate carbyne solid is still the subject of controversy (*6–8*). In the last few years, new features of the liquid state of C at low P have been discovered (*9–13*). In particular, C has been shown (*9*) to undergo a solid-liquid transition at $T = 4450$ K and $P \leq 4$ bars, leading to a metallic system. In two recent papers (*11,12*), we have discussed the bonding and electronic properties of low-P liquid C. The system has been found to be a good metal, composed of differently coordinated atoms (twofold, threefold, and fourfold), which display a variety of bonds from single to triple.

The high-P and high-T regions of the C phase diagram, whose characterization is of the greatest importance in astrophysics and geology, are largely unknown. The location of the solid-liquid phase boundary is in question (*1*), and the properties of the high-P liquid state have not yet been investigated. Many questions are unanswered, for example, whether C is solid or liquid in outer planets such as Uranus and Neptune (*5*) (where C is believed to be at $P \simeq 6$ Mbar and $T \simeq 7000$ K), and which phases of C are present in the mantle of Earth (*2*). Furthermore, the knowledge of the high-P equation of state of C is relevant to the conditions accessible in anvil cells (*14*) and to the prediction of the detonation properties of high explosives (*15*).

Diamond melting, indirectly supported by work done in the 1960s (*16*), was confirmed only in 1984 with direct evidence from experiments with diamond anvil cells (*14*). From the results of Bundy (*16,17*) and by analogy with the melting behavior of Si and Ge, many investigators (*1*) assumed that the diamond melting curve has a negative dP/dT slope (*18*). However, recent experiments (*3, 19–22*) indicate that the melting temperature (T_m) of diamond increases with pressure.

In this work, we present a first-principles molecular dynamics (MD) simulation (*23*) of diamond and liquid C at high P. We establish the sign of the slope dP/dT of the phase boundary, using the Clapeyron equation, and direct calculations of the change in P upon melting at constant volume. Furthermore, we investigate the bonding and structural properties of the high-P liquid state of C.

In our simulations, the interatomic potential is derived ab initio from the total energy of interacting ions and electrons, as described within density functional theory (DFT), in the local density approximation (*24*) (LDA). Since DFT has proven to be a valuable tool for the investigation of different forms of C, such as diamond (*25,26*), graphite (*27–29*), high-P metallic phases (*30, 31*), and amorphous C (*32*), our calculation of thermodynamic properties is expected to treat accurately the complex bonding characteristics of C and allow for realistic predictions of unknown properties in the solid and liquid states.

Melting and equilibration of C in the solid and liquid phases have been achieved with a constant-volume and constant-temperature MD method (*11, 12, 33, 34*). In our calculation, we used a supercell containing 64 atoms and 256 valence electrons, with simple cubic periodic boundary conditions (*35*). The P has been obtained for different temperatures from the expression:

$$P = \left\langle -\frac{\partial E}{\partial \Omega} \right\rangle + \rho_d K_B T \qquad (1)$$

where $\langle\ \rangle$ denotes temporal averages; E is energy; K_B is the Boltzmann constant; Ω is the volume of the system and ρ_d is its macroscopic density, which has been fixed at a value of 4.4 g cm^{-3}, corresponding (*36*) to a computed pressure of 0.6 Mbar for the solid at $T = 0$.

In order to determine the sign of dP/dT, we measured P as a function of T in the solid and liquid phases, at constant volume (*37*) (Fig. 1). We defined our system to be in the liquid phase when the atomic displacement as a function of the simulation time showed a diffusive behavior. As expected in classical systems, P varies almost linearly with T, in both the solid and the liquid. The crossing point of the two curves in Fig. 1 is at a very high T: 17,000 K. Therefore, provided that melting occurs at $T \leq 17{,}000$ K, we expect the difference in P between the liquid and the unstable solid to be positive at the melting point. Clearly, 17,000 K is much higher than any reasonable estimate for T_m. In fact, we can unambiguously establish that, already at $T \geq 8000$ K, the system is unstable toward melting.

We show this as follows. After 2000 MD steps at 8000 K, during which no diffusive behavior was observed, we removed one atom from the system, minimized the energy of the electronic states, and continued the calculation for another 2000 steps. In this way, we could measure the formation energy of a vacancy, which turned out to be very close to zero, to indicate an instability of the system toward spontaneous creation of vacancies. Had we continued the 63-atom run at 8000 K, we expect that a melting transition would have been ob-

---

G. Galli and R. M. Martin, Department of Physics and Material Research Laboratory, University of Illinois, Urbana, IL 61801.
R. Car, International School for Advanced Studies, Strada Costiera 11, 34014 Trieste, Italy.
M. Parrinello, IBM Research Division, Research Laboratory Zurich, CH-8803 Rüschlikon, Switzerland.

---

*Present address: IBM Research Division, Research Laboratory Zurich, CH-8803 Rüschlikon, Switzerland.

served, nucleated by the presence of the vacancy. However, in order to expedite matters, we further increased T to 9000 K. At this temperature, a spontaneous melting was observed after only 3000 steps. Figure 2 shows the mean-squared displacement of the atoms relative to the initial configuration and the time evolution of the P operator. Melting occurred very rapidly, in a first-order fashion, and the onset of the diffusive behavior was accompanied by a sudden rise in the P.

This result indicates that P increases as the material goes from solid to molten diamond, consistent with the results shown in Fig. 1.

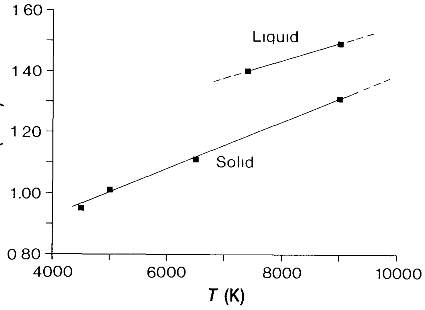

Fig. 1. Pressure (P) as a function of temperature (T) in the solid and liquid phases of C. We obtained the liquid at 9000 K by heating the 8000 K sample (see text), whereas we generated the liquid at 7500 K by cooling down the 9000 K system.

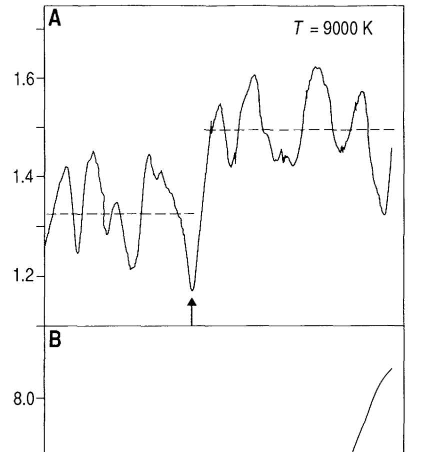

Fig. 2. Evolution of the pressure (P) operator (**A**) and mean squared displacement (r^2) of the atoms relative to the initial configuration (**B**), as a function of simulation time. Arrows indicate the onset of diffusive behavior (see text).

Therefore, in a constant-P transition the system must expand ($\Omega_\ell > \Omega_s$). If we assume that entropy (S) increases upon melting, from the Clapeyron equation:

$$\frac{dP}{dT} = \frac{S_\ell - S_s}{\Omega_\ell - \Omega_s} \tag{2}$$

we can conclude that dP/dT is positive. Thus, unlike the case of Si and Ge, liquid C is found to be less dense than diamond. Our findings are in agreement with shock wave data reported by Shaner *et al.* (*19, 20*), with the results of laser-heated diamond anvil cells presented by Bassett (*21*), with the results of transmission electron microscopy (*2*), and with recent resistance measurements (*22*) of diamond melts. They are in disagreement with the old picture of the C phase diagram (*1, 16, 17*), which predicted a negative slope for the diamond–liquid C phase line. Our results imply that, in the range of P and T thought to occur in Earth's mantle and in outer planets, any free C is solid and very likely in the diamond structure.

It would be of the greatest interest to explore the possibility of a change in slope of the diamond–liquid C phase boundary, at higher P, and the existence of new high-T phases.

Our results indicate that 8000 K is an upper bound to the diamond T_m. A precise determination of T_m involves a lengthy calculation of free energies in the solid and liquid phases. Although feasible, this would be very costly. However, an analysis of the particle-particle correlation functions (*38*) [$g(r)$] computed at different temperatures allows us to roughly estimate a lower bound for T_m of 6500 K. Figure 3 shows the $g(r)$ obtained at 6500 K and compares it with the corresponding one calculated at 8000 K, where the system is unstable. The system at 6500 K exhibits well-defined peaks (which correspond to the first-, second-, and third-neighbor distances of the diamond lattice, respectively), with no tendency toward melting, in contrast to the broad merging peaks found for the 8000 K sample. This suggests that at 6500 K the system is most likely still in the solid phase.

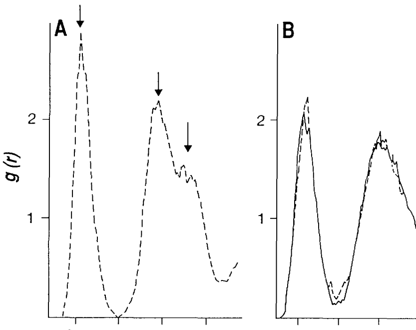

Fig. 3. Pair correlation functions (*39*) [$g(r)$] of diamond at (**A**) T = 6500 K and (**B**) T = 8000 K. Arrows in (A) indicate the first-, second-, and third-neighbor distances of the diamond lattice, respectively. In (B), the $g(r)$ obtained for the 64-atom system (solid line) is compared to that calculated for the system with a vacancy (dotted line) (see text).

The two liquids generated at 7500 and 9000 K have nearly identical properties. Their average coordination is close to 4, as in diamond, but their bonding properties are considerably different from those of the solid. Indeed, only 40 to 50% of the sites are fourfold coordinated; the remaining atoms are three- and fivefold coordinated and are present in approximately equal proportions. In contrast, the low-P liquid at T = 5000 K was found (*11, 12*) to have an average coordination slightly less than that of graphite (a threefold coordinated solid), with a considerable proportion of twofold atoms (32%), a small proportion of fourfold sites (16%), and about 50% distorted sp^2 units. The wide range of nearest-neighbor (N-N) distances (from those of the C_2 molecule to those of the diamond lattice) found in both the low- and the high-P liquids indicates that a variety of bonds, from sp to sp^3, are present in the two systems. However, the different kinds of coordination of the two melts suggest that sp^x bonds, with $1 \le x \le 2$, are the majority in the low-P liquid, whereas sp^x bonds with $2 \le x \le 3$ are prevalent in the high-P system.

As expected, we find that in the high-P liquid threefold atoms have the shortest bond lengths, whereas the fivefold ones have the longest N-N distances. Furthermore, fivefold sites have the widest range of preferred bond distances, with no atom having five bonds of approximately equal length. This suggests that the presence of atoms more than fourfold coordinated is basically due to high-T fluctuations and is consistent with the results of LDA calculations (*30, 31*) at T = 0, showing no tendency for C to have coordination higher than 4 for $P \le 10$ Mbar. This behavior is also different from that of Si and Ge, which are sixfold coordinated liquids both at low and at high P (*39*).

REFERENCES AND NOTES

1. For a review, see, for example, F. P. Bundy, *Physica A* **156**, 169 (1989), and references therein.
2. J. S. Dickey, W. A. Bassett, J. M. Bird, M. S. Weathers, *Geology* **11**, 219 (1983).
3. M. S. Weathers and W. A. Bassett, *Phys. Chem. Minerals* **15**, 105 (1987).
4. D. A. Young and R. Groover, in *Shock Waves in Condensed Matter* (Elsevier, Amsterdam, 1988), p. 131.
5. M. Ross, *Nature* **292**, 435 (1981).

6. A. G. Whittaker, *ibid.* **276**, 695 (1978); *Science* **200**, 763 (1978); *ibid.* **229**, 485 (1985).
7. R. B. Heimann, J. Kleinman, N. M. Salansky, *Nature* **306**, 164 (1983).
8. P. P. K. Smith and P. R. Buseck, *Science* **216**, 984 (1982); *ibid.* **229**, 486 (1985).
9. J. Heremans, C. H. Olk, G. L. Eeseley, J. Steinbeck, G. Dresselhaus, *Phys. Rev. Lett.* **60**, 453 (1988), and references therein.
10. J. Steinbeck, G. Braunstein, M. S. Dresselhaus, T. Venkatesan, D. C. Jacobson, *J. Appl. Phys.* **58**, 4374 (1985).
11. G. Galli, R. M. Martin, R. Car, M. Parrinello, *Phys. Rev. Lett.* **63**, 988 (1989).
12. ———, *Phys. Rev. B*, in press.
13. J. Tersoff, *Phys. Rev. Lett.* **61**, 2879 (1989).
14. J. S. Gold, W. A. Bassett, M. S. Weathers, J. M. Bird, *Science* **225**, 921 (1984).
15. M. van Thiel and F. H. Ree, *J. Appl. Phys.* **62**, 1761 (1987).
16. F. P. Bundy, *J. Chem. Phys.* **38**, 631 (1963).
17. ———, *J. Geophys. Res.* **85**, 6930 (1980).
18. As pointed out by Dickey *et al.* (*2*), this might bring the T_m of C into the range of Earth's geotherm at depths greater than 1200 km, and liquid C could play an important role in the dynamics of Earth's mantle.
19. J. W. Shaner, J. M. Brown, C. A. Swenson, R. G. McQueen, *J. Phys. C* **8**, 235 (1984).
20. A. C. Mitchell, J. W. Shaner, R. N. Keeler, *Physica* **139**, 386 (1986).
21. W. A. Bassett, *Bull. Am. Phys. Soc.* **35**, 465 (1990).
22. M. Togaya, paper presented at the First International Conference on the New Diamond Science and Technology (Tokyo, 1988).
23. R. Car and M. Parrinello, *Phys. Rev. Lett.* **55**, 2471 (1985).
24. For a review, see S. Lundqvist and N. H. March, Eds., *Theory of the Inhomogeneous Electron Gas* (Plenum, New York, 1983).
25. M. T. Yin and M. L. Cohen, *Phys. Rev. B* **24**, 6121 (1981).
26. J. R. Chelikowsky and S. Louie, *ibid.* **29**, 3470 (1984).
27. M. T. Yin and M. L. Cohen, *ibid.*, p. 6996.
28. S. Fahy, S. Louie, M. L. Cohen, *ibid.* **34**, 1191 (1986), and references therein.
29. M. Posternak, A. Baldereschi, A. J. Freeman, E. Wimmer, M. Weinert, *Phys. Rev. Lett.* **50**, 761 (1983), and references therein.
30. R. Biswas, R. M. Martin, R. J. Needs, O. H. Nielsen, *Phys. Rev. B* **30**, 3210 (1984); *ibid.* **35**, 9559 (1987).
31. M. T. Yin and M. L. Cohen, *Phys. Rev. Lett.* **50**, 2006 (1983).
32. G. Galli, R. M. Martin, R. Car, M. Parrinello, *ibid.* **62**, 555 (1989).
33. S. Nosé, *Mol. Phys.* **52**, 255 (1984); *J. Chem. Phys.* **81**, 511 (1984).
34. W. Hoover, *Phys. Rev. A* **31**, 1695 (1985).
35. We have adopted a nonlocal pseudopotential [G. B. Bachelet, D. Hamman, M. Schluter, *Phys. Rev. B* **26**, 4199 (1982)] of the form suggested by L. Kleinman and D. M. Bylander [*Phys. Rev. Lett.* **48**, 1425 (1982)] to describe the interaction between core (1*s*) and valence electrons. The single particle orbitals at the Γ point of the Brillouin zone have been expanded in plane waves, with a cutoff of 35 Ry. Time evolution has been simulated with a time step of 10^{-16} s.
36. The equilibrium density of diamond is 3.5 g cm^{-3}.
37. As a check on our work, we compared with experiment our estimate of the linear expansion coefficient

$$\alpha = \frac{1}{3B}\left(\frac{\partial P}{\partial T}\right)_{\Omega}$$

where B is the bulk modulus, of solid diamond for T higher than the Debye temperature (2000 K). Assuming a weak dependence of B upon T, we can use $B(T = 0)$ in the expression of α. The calculated value, $\simeq 510^{-6}$ K^{-1}, is in satisfactory agreement with the experimental one of $\simeq 710^{-6}$ K^{-1}.
38. The expression is

$$g\,(r) = \sum_{i,j} g_{ij}\,(r)$$

where i and j denote the differently coordinated sites present in the system; $g_{i,j}$, is defined as the number of particles with coordination i per unit volume, found at a distance r from an origin site with coordination j.
39. I. Stich *et al.*, *Phys. Rev. Lett.* **63**, 2240 (1989).
40. This work was supported by NSF grant DMR86-12860 (G.G. and R.M.M.) and by the Scuola Internazionale Superiors di Studi Avanzati (SISSA)–Centro Interuniversitario Nord-Est per il Calcolo Applicato (CINECA) by collaborative project, under the sponsorship of the Italian Ministry for Public Education (R. C. and M. P.). The computational work was done at the National Center for Supercomputing Applications. We benefited from useful discussions with J. Belak, M. Grumbach, M. Ross, J. W. Shaner, M. S. Weathers, and R. Young.

6 August 1990; accepted 12 October 1990

Stable Isotopic Evidence for a Pedogenic Origin of Carbonates in Trench 14 near Yucca Mountain, Nevada

JAY QUADE AND THURE E. CERLING

Layered carbonate and silica encrust fault fractures exposed in Trench 14 near Yucca Mountain, site of the proposed high-level nuclear waste repository in southern Nevada. Comparison of the stable carbon and oxygen isotopic compositions of the fracture carbonates with those of modern soil carbonates in the area shows that the fracture carbonates are pedogenic in origin and that they likely formed in the presence of vegetation and rainfall typical of a glacial climate. Their isotopic composition differs markedly from that of carbonate associated with nearby springs. The regional water table therefore remained below the level of Trench 14 during the time that the carbonates and silica precipitated, a period probably covering parts of at least the last 300,000 years.

ONE OF THE CHIEF ASSUMPTIONS used to justify locating a high-level nuclear waste repository at Yucca Mountain is that the buried waste will remain well within the unsaturated zone for the next several hundreds of thousands of years, regardless of even large changes in water-table elevation in response to climate change. A serious challenge to the validity of this assumption was the discovery of a complex network of carbonate and silica fillings in the fractures associated with several faults bordering Yucca Mountain. The best known and the most controversial of these fracture fillings are located in Trench 14, which crosses the Bow Ridge fault (Fig. 1). The thick, well-layered, and well-indurated nature of the fillings caused immediate concern because of similarity in these respects to vein cements and travertines associated with springs (*1*) and because of the apparent Quaternary age of some of the carbonate (*2*). A spring origin would imply that there was a rise in the regional water table, presumably during glacial maxima, to at least the level of Trench 14. Trench 14 is about 150 m above the level of the proposed repository and 400 m above the water table. A return to glacial hydrologic conditions might then result in ground-water flooding of the repository and rapid transport of radionuclides to nearby discharge points, such as Trench 14.

There has been a substantial effort at establishing the origin of the fracture cements in Trench 14 (*1*). An alternate hypothesis to a spring origin is that the carbonates and silica formed in soils in the vadose zone for hundreds of thousands of years (*2*). In this case, meteoric water infiltrating through the fractures deposited carbonate and silica as a normal part of desert soil formation.

To test these two hypotheses, we compared the carbon and oxygen isotopic data from Trench 14 to those in modern desert soils. We sampled soils in settings where the water table has remained tens to hundreds of meters below the surface during pedogenesis and therefore where ground water has played no role in carbonate formation. We took special care to sample soils younger than 7000 years old in order to establish the relation between the isotopic composition in soil carbonate and modern vegetation and rainfall (*3*). Pack-rat midden and pollen evidence shows that the distribution of vegetation has not greatly changed in the region during that span (*4*). We sampled soils displaying weak Stage I morphology (*5*), a degree of development consistent with a mid-to-late Holocene age. Five accelerator dates on thin carbonate coatings from three representative soils yielded ages between 3820 and 820 years (Table 1) (*6*).

The $\delta^{13}C$ content of modern soil carbonate varies substantially with elevation (Fig. 2) because of variations in (i) the isotopic composition of desert plants and (ii) the proportion of atmospheric CO_2 in the des-

Department of Geology and Geophysics, University of Utah, Salt Lake City, UT 84112.